

FULLERENE AROMATICITY BY CIRCULENE-FLOWER COVERINGS

Aniela E. Vizitiu¹, Mircea V. Diudea^{1,}, Titus A. Beu¹
and Attila Bende²*

¹ Babes-Bolyai University, Cluj, Romania

² National Institute for R&D of Isotopic and Molecular Technologies, Cluj, Romania

Abstract

Fullerene aromaticity/stability induced by circulene-flower coverings is evaluated by quantum calculations and HOMA geometric index. Infrared simulated spectra suggest similar behavior of similarly tessellated classical or non-classical fullerenes.

Keywords: fullerenes, “ab initio” quantum calculations, aromaticity, IR simulated spectra, local and global aromaticity, fullerene stability.

1. Introduction

The “artificial” synthesis of fullerenes with desired tessellation is hoped to be achieved via circulene (bowl-shaped) flowers Fw, [ncore:(mpetal)n]. Among several flower-units already synthesized [1], coronene [6:6₆] and sumanene [6:(5,6)₃] are the most promising. The idea of increasing aromaticity/stability of fullerenes tessellated by disjoint flowers DFws, originates in the classical texts of Clar, which postulate disjoint benzenoid rings as a criterion for the existence of fully conjugated aromatic structures, predicted to be extremely stable, in the VB theory.

Using the ratio heat of formation HF to the HOMO-LUMO band gap as a rough measure of fullerene stability, we found those fullerenes, whose molecular graphs are tessellated with disjoint flowers, the most stable, in several sets of isomeric fullerenes [2].

The of two most stable isomers of the series C₄₀ show D₂ and D_{5d} symmetry. The isomer 39-D_{5d}, (according to the Atlas of Fullerenes [3]) is a lens of two disjoint corannulenic flowers [5:6₅]DFw, whose largest HOMO-LUMO gap (6.2594 eV) is supposed to originate in its disjoint flower structure. Despite the isomer 38-D₂ shows a slightly lower HF/atom (a measure of thermodynamic stability of a molecule) and lower strain energy, its gap is

* Corresponding Author: Mircea V. Diudea, Address: Arany Janos Str. 11, 400048 Cluj, Romania, Fax: +40-264-590818; E-mail: diudea@chem.ubbcluj.ro

significantly lower, implying a lower kinetic stability of this molecule in comparison to the isomer 39- D_{5d} , for which the lowest HF/gap ratio was recorded in this series.

In the series of C_{42} fullerenes, the best values: energetic, electronic, strain and HF/Gap ratio are shown by the isomer 45- D_3 . This structure is tiled by two sumanenic disjoint flowers [6:(5,6)₃]DFw, sumanene being a recently synthesized molecule [4]. Similar result was found in the series of C_{48} fullerenes: the isomer with D_{6d} symmetry, tessellated by two coronenic disjoint flowers [6:6₆]DFw, shows the largest gap (5.988 eV), this being a warranty for its stability. The strain energy (calculated in terms of POAV1 approach [5]) is here larger in comparison to the better ranked isomers, an argument in favor of the most important role of the HOMO-LUMO gap.

2. Structure Generation and PM3 Data

We designed DFw cages by using operations on maps [6], as implemented in our software CageVersatile [7]. The simplest case is the lens-type structure and next constructions follow the Platonic solids as the parent cages. We limit here the discussion to the small cages listed in Figure 1.

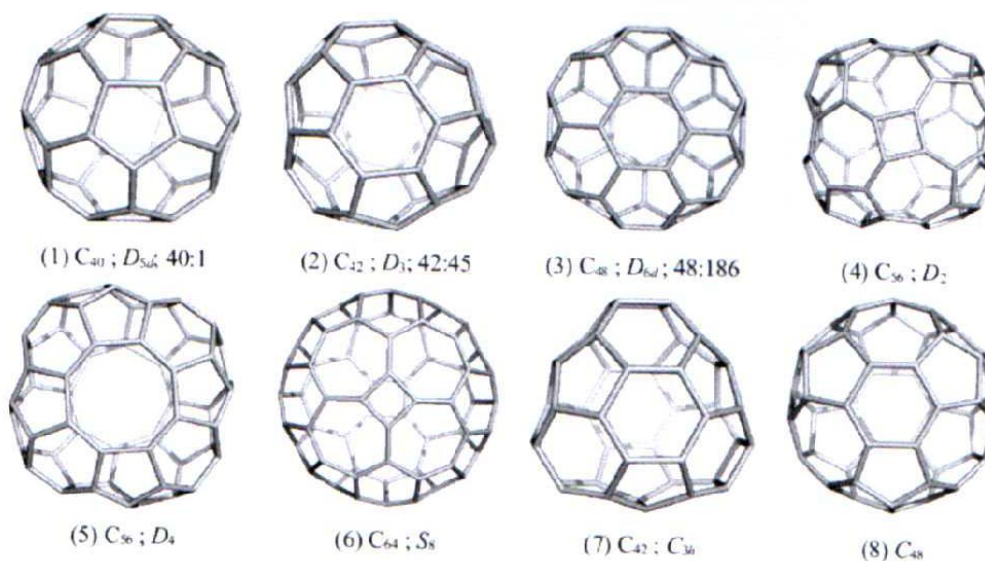
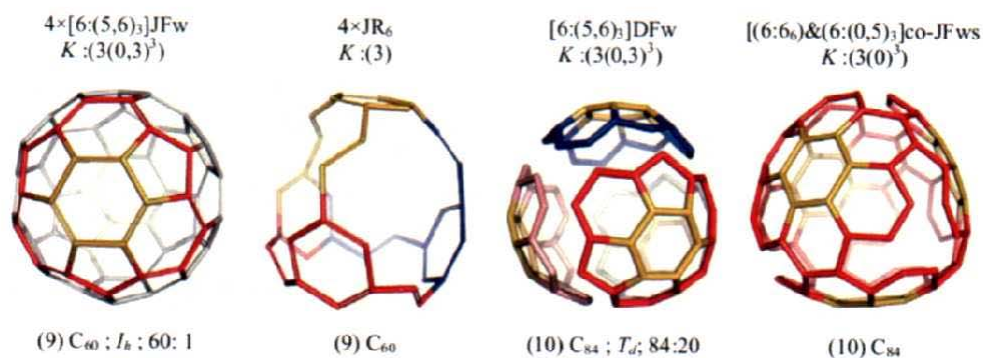


Figure 1. Small cages with disjoint flower DFw tessellation.

From the small classical (#1 to #3 and #8, numbered as in the Atlas of Fullerenes [3], see Table 1) and non-classical fullerenes (with faces other than pentagons and hexagons), the Buckminsterfullerene C_{60} and C_{84} (see Figure 2), both experimentally isolated fullerenes, are taken into consideration.

Table 1. PM3 data of different fullerene isomers

#	Structure	Sym	HF/at (eV) HF/Gap	Gap	SE/at Kcal/mol	HOMA /flower
1	C ₄₀ : 2×[5:6 ₅] [5]Corannulene	D _{5d}	20.628 14.302	6.2586	13.066	0.202
2	C ₄₂ : 2×[6:(5,6) ₃] [6]Sumanene	D ₃	19.676 14.449	5.908	12.329	-0.069
3	C ₄₈ : 2×[6:6] [6]Corannulene=Coronene	D _{6d}	21.972 15.923	5.988	12.612	0.049
4	C ₅₆ : 2×[4:(7(5c)) ₄] [c]Corazulene	D ₂	22.818 21.00	4.715	10.843	-0.225
5	C ₅₆ : 2×[8:(5,6) ₄] [8]Sumanene	D ₄	22.129 18.767	5.116	11.212	-0.375
6	C ₆₄ : 2×[4:(7(5d)) ₄] [d]Corazulene	S ₈	24.071 21.121	4.945	10.140	-0.930
7	C ₄₂ : 2×[6:(5,6) ₃] & 4x [4:6 ₄] [6]Sumanene	C _{3h}	20.534 13.346	6.6676	12.699	-0.1164
8	C ₄₈ : 2×[6:(5,7) ₃] [6]Corazene	C _{2h}	22.238 19.563	4.932	11.572	0.176

Figure 2. Sumanenic patterns in a tetrahedral embedding, as in C₆₀ (joint flower JFw) and C₈₄ (disjoint flower DFw) and their corresponding co-flowers.

3. DFT Calculations

Throughout the DFT calculations we have used the package GAUSSIAN 03 [8] for performing all-electron geometrical structure optimizations and subsequent IR-spectrum calculations for the considered fullerene cages.

We have investigating the appropriateness of the basis sets 6-31g and 6-31g(d). Both have proved to yield reliable and absolutely comparable results at reasonable computation costs. However, the usage of the polarized basis set 6-31g(d) has turned out to be too time-

consuming for the envisaged IR-spectrum calculations and we did not use it in the production calculations.

In order to adopt an appropriate exchange-correlation functional, we have compared the results obtained for the C_{60} fullerene with the widely used B3LYP functional [9] and with the more recent functional PBE-PBE [10]. The PBE-PBE functional reproduces well the experimental HOMO-LUMO gap of C_{60} (1.6-1.85 eV.), yielding 1.770 eV (1.668 eV) with the 6-31g (6-31g(d)) basis set and with the basis set, whereas the B3LYP functional seems to perform rather poorly, yielding 2.762 eV. Consequently, we have employed the PBE-PBE/6-31g combination throughout in the production calculations.

Table 2 shows the electronic structure results yielded by our DFT calculations. As can be easily seen, the HOMO-LUMO gap decreases monotonously from C_{40} to C_{56} . Interestingly, the gap for C_{84} is significantly larger than for the rest of the implied cages.

The simulated spectra are plotted in Fig. (3). For comparison purposes, in the lowest and topmost panel, also the spectrum of C_{60} was included. Except for C_{56} (D_4), the structure of the spectra is relatively simple, reflecting the high symmetry of the cages. Remarkably simple are the spectra for C_{40} , C_{48} , and C_{84} , which share the common feature that they belong to point groups characterized by dihedral reflections (D_{5d} , D_{6d} , and respectively, T_d).

Table 2. DFT electronic structure results for different fullerene isomers based on the PBE-PBE functional and the 6-31g basis set.

#	Structure	Total energy /atom (a.u.)	Symmetry	HOMO (a.u.)	HOMO-LUMO Gap (a.u.)
1	C_{40} : $2 \times [5:6_5]$	-38.051	D_{5d}	-0.195	0.037
2	C_{42} : $2 \times [6:(5,6)_3]$	-38.052	C_3	-0.195	0.033
3	C_{48} : $2 \times [6:6_6]$	-38.048	D_{6d}	-0.190	0.028
4	C_{56} : $2 \times [4:(7(5c))_4]$	-38.049	D_2	-0.161	0.024
5	C_{56} : $2 \times [8:(5,6)_4]$	-38.049	D_4	-0.176	0.017
10	C_{84} : $4 \times [6:(5,6)_3]$	-38.062	T_d	-0.199	0.060

Nearly all of the studied molecules show one of their most intense vibrations in the range 600-700 cm^{-1} (C_{42} : 646.9 cm^{-1} , $C_{56}D_4$: 671.1 cm^{-1} , C_{40} : 675.2 cm^{-1} , C_{48} : 670.0 cm^{-1}). These vibrations mainly arise from out-of-plane atomic motions and the involved atoms are located on the boundary of the discussed flowers. In the case of C_{84} , the low-frequency dominant normal mode is shifted towards even lower frequencies (513.2 cm^{-1}) due to the more massive neighborhood of the flowers.

Other major IR-active vibrations are located in the range 1250-1430 cm^{-1} . These types of vibrations characterize the atoms of flowers, and arise mainly from in-plane atomic motions; Figure 4 shows the displacement patterns of the most intense IR active modes.

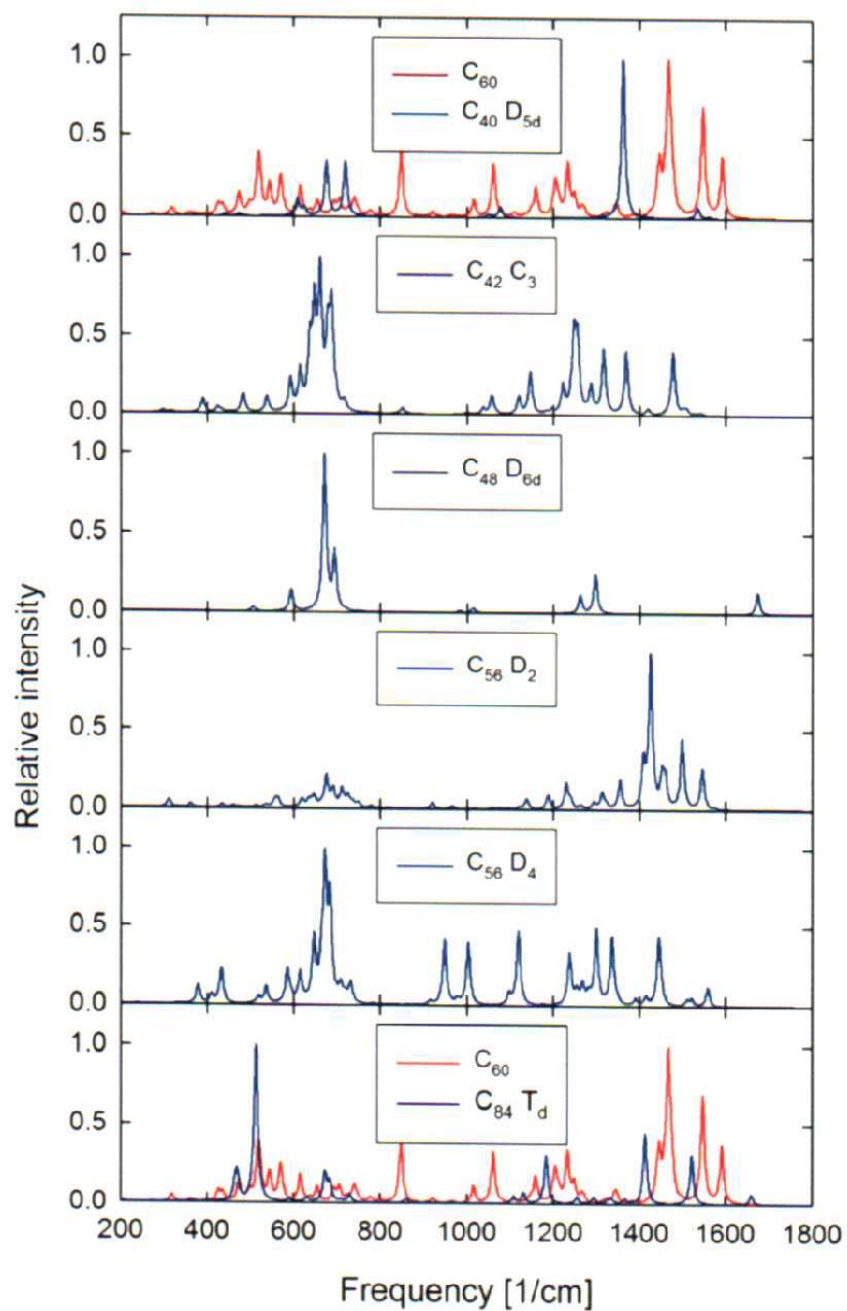


Figure 3. IR spectra of the fullerenes in Table 2 yielded by DFT calculations with the PBE-PBE functional / 6-31g basis set.

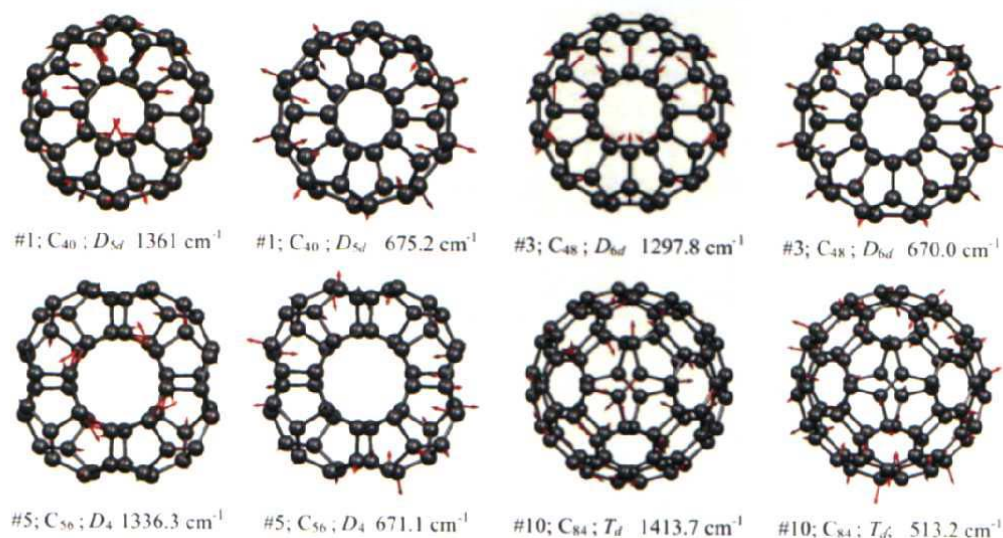


Figure 4. Most intense IR-active vibrational modes of the fullerenes in Table 2.

References

- [1] J. T. Craig, B. Halton and S. Lo, A new coronene synthesis, *Aust. J. Chem.* 1975, 28, 913-916; U. Rohr, Ch. Kohl, K. Müllen, A. van de Craats, and J. Warman, Liquid crystalline coronene derivatives, *J. Materials Chem.*, 2001, 11, 1789-1799; K. Yamamoto, Extended systems of closed helicene. Synthesis and characterization of [7] and [7.7]-circulene, *Pure Appl. Chem.* 1993, 65, 157-164; A. E. Vizitiu, Modeling molecular Structures and Properties by the aid of topological descriptors, PhD Thesis, Cluj, Romania, 2007.
- [2] P. W. Fowler and D. E. Manolopoulos, *An Atlas of Fullerenes*, Clarendon Press, Oxford, 1995.
- [3] H. Sakurai, T. Daiko, and T. Hirao, A synthesis of sumanene, a fullerene fragment, *Science*, 2003, 301, 1878-1878; H. Sakurai, T. Daiko, H. Sakane, T. Amaya, and T. Hirao, Structural Elucidation of Sumanene and Generation of its Benzylic Anions, *J. Am. Chem. Soc.*, 2005, 127, 11580-11581.
- [4] R. C. Haddon, Rehybridization and π -orbital overlap in nonplanar conjugated organic molecules: π -orbital axis vector (POAV) analysis and three-dimensional Hückel molecular orbital (3D-HMO) theory, *J. Am. Chem. Soc.*, 1987, 109, 1676-1685; R.C. Haddon, Hybridization as a Metric for the Reaction Coordinate of Chemical Reactions, *J. Am. Chem. Soc.*, 1998, 120, 10494-10496.
- [5] E. Vizitiu, M. V. Diudea, S. Nikolić and D. Janežić, Retro-Leapfrog and other retro map operations, *J. Chem. Inf. Model.*, 2006, 46, 2574-2578; M. V. Diudea, P. E. John, A. Graovac, M. Primorac, and T. Pisanski, Leapfrog and Related Operations on Toroidal Fullerenes, *Croat. Chem. Acta*, 2003, 76, 153-159;
- [6] M. V. Diudea, M. Ştefu, P. E. John, and A. Graovac, Generalized operations on maps, *Croat. Chem. Acta*, 2006, 79, 355-362.

-
- [7] M. Stefu and M. V. Diudea, CageVersatile 1.3, "Babes-Bolyai" University, 2003.
- [8] Gaussian 03, Revision B.05, M. J. Frisch, G. W. Trucks, H. B. Schlegel, G. E. Scuseria, M. A. Robb, J. R. Cheeseman, J. A. Montgomery, Jr., T. Vreven, K. N. Kudin, J. C. Burant, J. M. Millam, S. S. Iyengar, J. Tomasi, V. Barone, B. Mennucci, M. Cossi, G. Scalmani, N. Rega, G. A. Petersson, H. Nakatsuji, M. Hada, M. Ehara, K. Toyota, R. Fukuda, J. Hasegawa, M. Ishida, T. Nakajima, Y. Honda, O. Kitao, H. Nakai, M. Klene, X. Li, J. E. Knox, H. P. Hratchian, J. B. Cross, C. Adamo, J. Jaramillo, R. Gomperts, R. E. Stratmann, O. Yazyev, A. J. Austin, R. Cammi, C. Pomelli, J. W. Ochterski, P. Y. Ayala, K. Morokuma, G. A. Voth, P. Salvador, J. J. Dannenberg, V. G. Zakrzewski, S. Dapprich, A. D. Daniels, M. C. Strain, O. Farkas, D. K. Malick, A. D. Rabuck, K. Raghavachari, J. B. Foresman, J. V. Ortiz, Q. Cui, A. G. Baboul, S. Clifford, J. Cioslowski, B. B. Stefanov, G. Liu, A. Liashenko, P. Piskorz, I. Komaromi, R. L. Martin, D. J. Fox, T. Keith, M. A. Al-Laham, C. Y. Peng, A. Nanayakkara, M. Challacombe, P. M. W. Gill, B. Johnson, W. Chen, M. W. Wong, C. Gonzalez, and J. A. Pople, Gaussian, Inc., Pittsburgh PA, 2003.
- [9] D. Becke, Density-functional thermochemistry. III. The role of exact exchange, *J. Chem. Phys.*, 1993, 98, 5648-5652; C. Lee, W. Yang, and R. G. Parr, Development of the Colle-Salvetti correlation-energy formula into a functional of the electron density, *Phys. Rev. B*, 1988, 37, 785-789.
- [10] J. P. Perdew, K. Burke, and M. Ernzerhof, Generalized Gradient Approximation Made Simple, *Phys. Rev. Lett.*, 1996, 77, 3865-3868.